2018 IEEE Conference on Decision and Control (CDC)
Miami Beach, FL, USA, Dec. 17-19, 2018

A Network Optimization Framework for the Analysis and Control of Traffic Dynamics and Intersection Signaling

Gianluca Bianchin and Fabio Pasqualetti

Abstract— **This paper proposes a simplified version of classical models for urban transportation networks, and studies the problem of controlling intersections with the goal of optimizing network-wide congestion. Differently from traditional approaches to control traffic signaling, our simplified framework allows a more tractable analysis of the network dynamics and, yet, accurately captures the behavior of traffic flows along roads and in proximity of intersections in regimes of free flow. We cast an optimization problem to describe the goal of optimally controlling automated intersections, and relate congestion objectives with the problem of optimizing a metric of controllability of the associated dynamical system. We characterize the system performance in relation to (sub)optimal configurations, and identify conditions that guarantee network stability. Lastly, we assess the benefits of the proposed modeling and optimization framework through a microscopic simulator.**

I. Introduction

Effective control of transportation systems is at the core of the smart city paradigm, and has the potential for improving efficiency and reliability of urban mobility. Modern urban transportation architectures comprise two fundamental components: traffic intersections and interconnecting roads. Intersections connect and regulate conflicting traffic flows among adjacent roads, and their effective control can prevent congestion and sensibly improve travel time. Congestion is the result of limits in the capacity of the network, and often leads to degraded network throughput and user travel time.

In this paper, we propose a simplified modeling paradigm that captures the space-time relations between adjacent intersections, and sets out as a tractable framework to study efficiency and reliability of this class of dynamical systems. The proposed framework is employed in this work for the control of green split times at intersections.

Related Work: The design of feedback policies for the control of urban infrastructures is an intensively studied topic. The proposed techniques can mainly be divided into two categories: routing policies and intersections control. Routing policies use a combination of turning preferences and speed limits in order to optimize congestion objectives, and have been studied both in a centralized and distributed framework [1], [2]. Conversely, intersections control refers to the design of the scheduling of the (automated) intersections so that the intersection capacity is maximized, and can be achieved: i) by controlling the signaling sequence and offset, and/or ii) by designing the signaling durations. The control of signal offsets typically aims at tuning the synchronization of adjacent intersections in order to produce green-wave effects [3]. In contrast, the duration of green times at intersections impacts the network overall traffic flows, and plays a significant role in the efficiency of large-scale networks [4].

Widely-used distributed signaling control methods include SCOOT [5], RHODES [6], OPAC [7], and emerge as the most common methods currently employed in major cities. The sub-optimal performance of the above methods [8] has motivated the development of max-pressure techniques [9]. Max-pressure methods use a store-and-forward model where queues at intersections have unlimited queue lengths. Under this assumption, max pressure is proven to maximize the throughput by stabilizing the network. Centralized policies require higher modeling efforts, but in general have better performance guarantees [10]. Among the centralized policies, the Traffic-Responsive Urban Control framework [4] has received considerable interest for its simplicity and performance. The high complexity of traffic networks has recently motivated the development of simplified (averaged) models to deal with the switching nature of the traffic signals [11]. However, the highly-nonlinear behavior of this class of dynamical systems still limits our capability to consider adequate optimization and prediction horizons, and the development of tractable models capable of capturing all the relevant network dynamics is still an open problem.

Contribution: This paper proposes a simplified modeling paradigm that describes the spatial and temporal behavior of the overall network traffic flows. With respect to established models, our framework relies on a continuous time and discrete space characterization of the flows, and allows for a more tractable network analysis. We employ this model to formalize the goal of optimally designing green split durations, and provide a relation to the optimization of a metric of controllability of a dynamical system associated with the network. We employ the concept of smoothed spectral abscissa [12] to numerically solve this optimization problem, and we demonstrate the benefits of the method through a microscopic simulator. Our results show that the increment in complexity deriving from a global model description is justified by the increased system performance.

Organization: Section II describes the problem setup, relates our modeling framework to previously-established traffic models, and formulates the problem of minimizing network congestion by selecting the duration of the green times at intersections. Section III illustrates the proposed numerical approach to solve the optimization. Section IV is

This material is based upon work supported in part by ARO award 71603NSYIP, and in part by NSF award CNS1646641. Gianluca Bianchin and Fabio Pasqualetti are with the Mechanical Engineering Department, University of California, Riverside, {gianluca, fabiopas}@engr.ucr.edu.

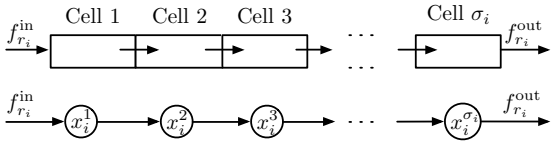

Fig. 1. Road discretization and corresponding network model. The portion of road comprised between spatial coordinates s_{k-1} and s_k, $k \in \{1, \dots, \sigma_i\}$ is referred to as cell k, and variable x_i^k denotes the cell density.

devoted to numerical simulations that validate our assumptions and the solution method. Section V concludes the paper.

II. Dynamical Model of Traffic Networks and Problem Formulation

We model urban traffic networks as a set of one-way roads interconnected through signalized intersections. Within each road, vehicles move at the free-flow velocity, while traffic flows are exchanged between adjacent roads by means of the signalized intersection connecting them. In this section, we discuss a concise dynamical model for traffic networks.

A. Model of Road and Traffic Flow

Let $\mathcal{N} = (\mathcal{R}, \mathcal{I})$ denote a traffic network with roads $\mathcal{R} = \{r_1, \dots, r_{n_r}\}$ and intersections $\mathcal{I} = \{\mathcal{I}_1, \dots, \mathcal{I}_{n_\mathcal{I}}\}$. Each element in the set $\mathcal{R}$ models a one way (multi-lane) road, whereas intersections regulate conflicting flows of traffic among adjacent roads (see Section II-B). We assume that exogenous inflows enter the network at (source) roads $\mathcal{S} \subseteq \mathcal{R}$ and, similarly, outflows exit the network at (destination) roads $\mathcal{D} \subseteq \mathcal{R}$, with $\mathcal{S} \cap \mathcal{D} = \varnothing$. To avoid trivial cases, we assume that there exists a path in $\mathcal{N}$ from every road in $\mathcal{R}$ to at least one destination in $\mathcal{D}$. We let $\ell_i \in \mathbb{R}$ denote the length of road r_i, and we discretize each r_i into $\sigma_i = \lceil \ell_i / h \rceil$ cells [13], where the parameter $h \in \mathbb{R}_{>0}$ is a constant discretization step (see Fig. 1). We denote by $x_i^k \in \mathbb{R}$ the traffic density within the k-th cell of road r_i, $k \in \{1, \dots, \sigma_i\}$. We assume that the flow of vehicles $f^{\text{in}}_{r_i}$ enters road r_i in correspondence of cell $k = 1$; accordingly, the flow $f^{\text{out}}_{r_i}$ leaves the road in correspondence of cell $k = \sigma_i$. We model the relation between traffic flows and cell densities by assuming that vehicles move along the road with constants velocity γ_i, the average (free-flow) speed along the link. We model the dynamics of the road state $x_i = [x_i^1 \ \cdots \ x_i^{\sigma_i}]^\mathsf{T}$ as

$$\begin{bmatrix} \dot{x}_i^1 \\ \dot{x}_i^2 \\ \vdots \\ \dot{x}_i^{\sigma_i} \end{bmatrix} = \underbrace{\frac{\gamma_i}{h} \begin{bmatrix} -1 & & & \\ 1 & -1 & & \\ & \ddots & \ddots & \\ & & 1 & 0 \end{bmatrix}}_{D_i} \begin{bmatrix} x_i^1 \\ x_i^2 \\ \vdots \\ x_i^{\sigma_i} \end{bmatrix} + \begin{bmatrix} f^{\text{in}}_{r_i} \\ 0 \\ \vdots \\ -f^{\text{out}}_{r_i} \end{bmatrix}. \quad (1)$$

Remark 1: ***(Equivalence between*** (1) ***and hydrodynamic models)*** The dynamical model (1) can be derived from the mass-conservation continuity equation [13], in certain traffic regimes. Let the function $\rho_i = \rho_i(s,t) \geq 0$ denote the (continuous) density of vehicles within road r_i at the spatial coordinate $s \in [0, \ell_i]$ and time $t \in \mathbb{R}_{\geq 0}$, and $f_i = f_i(s,t) \geq 0$ the (continuous) flow of vehicles along the road. Traffic densities and flows follow the hydrodynamic relation

$$\frac{\partial \rho_i}{\partial t} + \frac{\partial f_i}{\partial s} = 0.$$

We first complement the above continuity equation with the Lighthill-Whitham-Richards static relation, $f_i = f_i(\rho_i)$, in which traffic flows instantaneously change with the density. Then, we include the speed-density fundamental relation $f_i = \rho_i v(\rho_i)$, where $v : \mathbb{R}_{\geq 0} \to \mathbb{R}_{\geq 0}$ represents the speed of the traffic flow, to obtain

$$\frac{\partial \rho_i}{\partial t} + \left(v(\rho_i) + \rho_i \frac{d\ v(\rho_i)}{d\rho_i} \right) \frac{\partial \rho_i}{\partial s} = 0.$$

Solutions to the above relation are kinematic waves [13] moving at speed $\gamma(\rho_i) = v(\rho_i) + \rho_i \frac{dv(\rho_i)}{d\rho_i}$. We consider scenarios where the speed of the kinematic wave can be approximated as $\gamma(\rho_i) \approx \gamma_i$, where γ_i is a constant. As discussed in [13], this approximation is accurate in regimes of free flow, characterized by $\frac{dv(\rho_i)}{d\rho_i} \approx 0$. Therefore, we let γ_i denote the average speed of the flow along the link, and consider the approximated continuity equation

$$\frac{\partial \rho_i}{\partial t} + \gamma_i \ \frac{\partial \rho_i}{\partial s} = 0.$$

We then discretize in space the the above relation by: (i) considering the discrete spatial coordinate

$$s_k = kh, \qquad k \in \{0, \dots, \sigma_i\},$$

and by (ii) replacing the partial derivative with respect to s with the difference term

$$\frac{\partial \rho_i(s_k, t)}{\partial t} = -\gamma_i \ \frac{\rho_i(s_k, t) - \rho_i(s_{k-1}, t)}{h}.$$

Under classical conditions on the discretization step h [13], this discretization leads to the dynamical model (1), after introducing the boundaries conditions $f^{\text{in}}_{r_i}$ and $f^{\text{out}}_{r_i}$, and by replacing $\rho_i(s_k, t)$ with the compact notation x_i^k. □

B. Model of Intersection and Interconnection Flow

Signalized intersections alternate the right-of-way of vehicles to coordinate and secure conflicting flows between adjacent roads. Every signalized intersection $\mathcal{I}_j \in \mathcal{I}$, $j \in \{1, \dots, n_\mathcal{I}\}$, is modeled as a set $\mathcal{I}_j \subseteq \mathcal{R} \times \mathcal{R}$, consisting of all allowed movements between intersecting roads. For road $r_i \in \mathcal{R}$, let $\mathcal{I}^{r_i}_{\text{in}}$ denote the (unique) intersection at the road upstream. Similarly, let $\mathcal{I}^{r_i}_{\text{out}}$ denote the (unique) intersection at the road downstream. Then, road inflows and outflows can be modeled as

$$\begin{aligned} f^{\text{in}}_{r_i} &= \sum_{(r_i, r_k) \in \mathcal{I}^{r_i}_{\text{in}}} s(r_i, r_k, t)\, f(r_i, r_k) + u_{r_i}, \\ f^{\text{out}}_{r_i} &= \sum_{(r_k, r_i) \in \mathcal{I}^{r_i}_{\text{out}}} s(r_k, r_i, t)\, f(r_k, r_i) + w_{r_i}, \end{aligned} \quad (2)$$

where $f : \mathcal{R} \times \mathcal{R} \to \mathbb{R}_{\geq 0}$ denotes the intersection transmission rate, which is controlled over time by the green split function $s : \mathcal{R} \times \mathcal{R} \times \mathbb{R}_{\geq 0} \to \{0, 1\}$. We incorporate exogenous inflows and outflows to the road (flows that are not originated or merge to modeled intersections or roads)

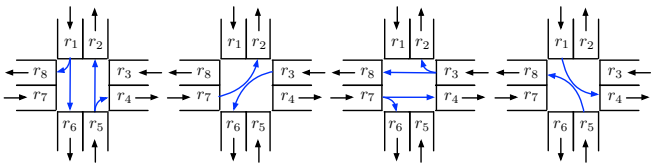

Fig. 2. Typical set of phases at a four-ways intersection.

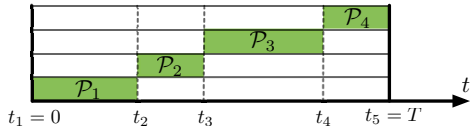

Fig. 3. Green splits for the four ways intersection in Fig. 2.

into $f^{\text{in}}_{r_i}$ and $f^{\text{out}}_{r_i}$ respectively, by defining the input term $u_{r_i} : \mathbb{R}_{\geq 0} \to \mathbb{R}_{\geq 0}$ and output term $w_{r_i} : \mathbb{R}_{\geq 0} \to \mathbb{R}_{\geq 0}$. For all $r_i \in \mathcal{R}$, $u_{r_i} \neq 0$ if and only if $r_i \in \mathcal{S}$, while $w_{r_i} \neq 0$ if and only if $r_i \in \mathcal{D}$. The notation $f(r_i, r_k)$ represents the transmission rate from road r_k to r_i.

Example 1: ***(Green split functions)*** Consider the four-ways intersection in Fig. 2. The intersection is modeled as

$$\tilde{\mathcal{I}} = \{(r_1, r_6), (r_1, r_8), (r_5, r_2), (r_5, r_4), (r_7, r_2), (r_3, r_6), (r_3, r_8), (r_3, r_2), (r_7, r_4), (r_7, r_6), (r_5, r_8), (r_1, r_4)\}.$$

It is common to associate to $\tilde{\mathcal{I}}$ a set of four phases $\mathcal{P}_1 = \{(r_1, r_6), (r_1, r_8), (r_5, r_2), (r_5, r_4)\}$, $\mathcal{P}_2 = \{(r_7, r_2), (r_3, r_6)\}, \mathcal{P}_3 = \{(r_3, r_8), (r_3, r_2), (r_7, r_4), (r_7, r_6)\}, \mathcal{P}_4 = \{(r_5, r_8), (r_1, r_4)\}$. The green split function for the intersection is defined by alternating the set of available phases within a cycle time $T \in \mathbb{R}_{\geq 0}$, that is, for all $j \in \{1, \dots, 4\}$,

$$s(r_i, r_k, t) = \begin{cases} 1 & \text{if } (r_i, r_k) \in \mathcal{P}_j \text{ and } t \in [t_j, t_{j+1}), \\ 0 & \text{otherwise,} \end{cases}$$

and it is commonly graphically represented as in Fig. 3. □

We assume that road outflows are functions proportional to the density of the downstream cell, and let

$$f(r_i, r_k) = c(r_i, r_k) x_k^{\sigma_k}, \tag{3}$$

where $c : \mathcal{R} \times \mathcal{R} \to \mathbb{R}$ is a parameter that models the speed of the outflow, captures the fact that queues may have different departing rates, and includes the (constant) average routing ratio of vehicles wishing to enter road r_i from r_k.

Remark 2: ***(Transmission rates)*** In the transportation literature, the traffic flow through an intersection often includes a saturation term of the form:

$$f(r_i, r_k) = \min\{\bar{f}, c(r_i, r_k) x_k^{\sigma_k}\},$$

where $\bar{f} \in \mathbb{R}_{>0}$ denotes the intersection saturation flow. In this work we consider regimes of free-flow where (3) is a valid approximation of the above nonlinear relation. □

C. Switching and Time-Invariant Traffic Network Dynamics

We combine individual roads dynamics into a joint model that describes the overall network interconnection. By substituting (2) and (3) into (1), we obtain

$$\underbrace{\begin{bmatrix} \dot{x}_1 \\ \dot{x}_2 \\ \vdots \\ \dot{x}_{n_r} \end{bmatrix}}_{\dot{x}} = \underbrace{\begin{bmatrix} A_{11} & A_{12} & \cdots & A_{1n_r} \\ A_{21} & A_{22} & \ddots & A_{2n_r} \\ \vdots & \ddots & \ddots & \vdots \\ A_{n_r1} & A_{n_r2} & \cdots & A_{n_rn_r} \end{bmatrix}}_{A} \underbrace{\begin{bmatrix} x_1 \\ x_2 \\ \vdots \\ x_{n_r} \end{bmatrix}}_{x} + \underbrace{\begin{bmatrix} I_{n_1} & 0 & \cdots & 0 \\ 0 & I_{n_2} & \ddots & 0 \\ \vdots & \ddots & \ddots & \vdots \\ 0 & 0 & \cdots & I_{n_r} \end{bmatrix}}_{B} \underbrace{\begin{bmatrix} u_1 \\ u_2 \\ \vdots \\ u_{n_r} \end{bmatrix}}_{u}, \tag{4}$$

where $A \in \mathbb{R}^{n \times n}$, $n = \sum_{i=1}^{n_r} \sigma_i$,

$$A_{ik} = \begin{cases} s(r_i, r_k, t) c(r_i, r_k) e_1 e_{\sigma_k}^{\mathsf{T}}, & \text{if } i \neq k, \\ D_i - (\sum_\ell s(r_\ell, r_i, t) c(r_\ell, r_i) + \bar{w}_{r_i}) e_{\sigma_i} e_{\sigma_i}^{\mathsf{T}}, & \text{if } i = k, \end{cases}$$

and $e_i \in \mathbb{R}^{\sigma_i}$ denotes the i-th canonical vector of length σ_i. We adopt an approach similar to [14], and assume that exogenous outflows are proportional to the number of vehicles in the road, that is, $w_{r_i} = \bar{w}_{r_i} x_i^{\sigma_i}$, $\bar{w}_{r_i} \in [0, 1]$.

The network model (4) represents a linear switching system, where the switching signals are the green split functions $s(r_i, r_k, t)$ at the intersections. It is worth noting that the matrix A in (4) is typically sparse, because not all roads are adjacent, and its sparsity pattern varies over time as determined by the green splits $s(r_i, r_k, t)$.

Example 2: ***(Example of traffic network)*** Consider the network illustrated in Fig. 4, with $\mathcal{R} = \{r_1, \dots, r_{12}\}$ and $\mathcal{I} = \{\mathcal{I}_1, \dots, \mathcal{I}_4\}$. The network comprises four destination roads $\mathcal{D} = \{r_2, r_5, r_8, r_{11}\}$, with $\bar{w}_{r_i} = 1$ for all $r_i \in \mathcal{D}$, and four source roads $\mathcal{S} = \{r_1, r_3, r_{10}, r_{12}\}$, with $u_{r_i} \neq 0$ for all $r_i \in \mathcal{S}$. Let $\ell_i/h = 3$ and $\gamma_i/h = 3$ for all $i \in \{1, \dots, n_r\}$. Then, (4) reads as

$$A_{ii} = \begin{bmatrix} -1 & & \\ 1 & -1 & \\ & 1 & -(\sum_\ell s(r_\ell, r_i, t) c(r_\ell, r_i) + \bar{w}_{r_i}) \end{bmatrix},$$

$$A_{ij} = \begin{bmatrix} 0 & 0 & s(r_i, r_j, t) c(r_i, r_j) \\ 0 & 0 & 0 \\ 0 & 0 & 0 \end{bmatrix},$$

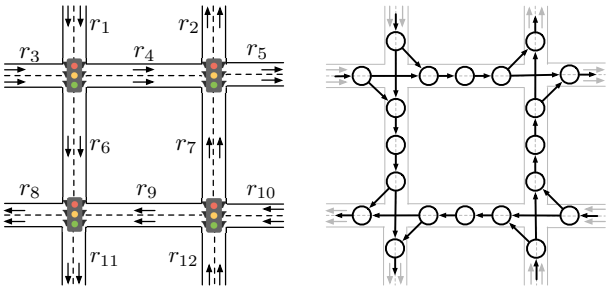

(a) (b)

Fig. 4. Network model associated with a traffic network composed of $n_{\mathcal{I}} = 4$ intersections and $n_r = 12$ roads. Each road is associated with a set of states that represent the density of the cells within the roads.

for all $i, j \in \{1, \dots, n_{\mathrm{r}}\}$. Notice that we let $s(r_i, r_j, t) = 0$ for all times if $(r_j, r_k) \notin \mathcal{I}_k$ for all $k \in \{1, \dots, n_{\mathcal{I}}\}$. □

We make the assumption that all scheduling functions are periodic with period T. That is, for all $(r_i, r_k) \in \mathcal{I}_j$, $j \in \{1, \dots, n_{\mathcal{I}}\}$, and for all times $t \in \mathbb{R}_{\geq 0}$,

$$s(r_i, r_k, t) = s(r_i, r_k, t + T).$$

Let $\mathcal{T} = \{\tau_1, \dots, \tau_m\}$ denote the set of time instants in the interval $[0, T]$ when a scheduling function changes its value:

$$\mathcal{T} = \{\tau \in [0, T] \ : \ \exists (r_i, r_k) \in \mathcal{I}, \lim_{t \to \tau^-} s(r_i, r_k, t) \neq \lim_{t \to \tau^+} s(r_i, r_k, t)\}.$$

Notice that the matrix A in (4) remains constant between any consecutive time instants τ_{i-1} and τ_i. We denote such matrix with A_i, and refer to it as to the i-th network mode. Let $d_i = \tau_i - \tau_{i-1}$, with $i \in \{1, \dots, m\}$ and $\tau_0 = 0$, denote the duration of the i-th network mode. We define a linear-time invariant approximation of the switching dynamics (4):

$$\dot{x}_{\mathrm{av}} = A_{\mathrm{av}} x_{\mathrm{av}} + Bu, \tag{5}$$

where $A_{\mathrm{av}} = \frac{1}{T} \sum_{i=1}^{m} d_i A_i$, x_{av} describes the average traffic densities along the roads over the period T. We observe that the average dynamics are obtained by considering the average durations of the split signals over the period T, and that the averaging technique preserves the sparsity pattern of the network in the average dynamics (5). That is, $A_{\mathrm{av}}(i, j) \neq 0$ if and only if $A_k(i, j) \neq 0$ for some $k \in \{1, \dots, m\}$.

Remark 3: ***(Assumptions leading to average dynamics)*** The average network dynamics (5) can be obtained from the state-space averaging technique [15]. The approximation of the behavior of the switched system (4) with the average dynamics (5) is valid if the following approximation holds:

$$e^{A_1 d_1} e^{A_2 d_2} \dots e^{A_m d_m} \approx e^{A_1 d_1 + \dots + A_m d_m}.$$

State-space averaging is appealing because of its mathematical simplicity, and it gives satisfactory results if the operating period T is short in comparison to the system dynamics. Fig. 5 presents a comparison of the time-evolution of road densities between a microscopic simulation (continuous line), and the average dynamics (5) (dashed lines), for the network discussed in Example 2. As (qualitatively) illustrated in the figure, a precise choice for the outflow rates $c(r_i, r_k)$ allows the time evolution of (5) (dashed lines) to approximate the microscopic queues behavior (continuous lines). □

D. Problem Formulation

In this paper, we consider the dynamical model (5) and focus on the problem of designing the durations of the green split functions so that a measure of network congestion is minimized. The average model (5) allows us to design the durations of the modes rather than their exact sequence. Thus, similarly to e.g. [3], we adopt a two-stage optimization process. First, we design the optimal durations of the modes by taking into account the overall network dynamics. Second, a (possibly distributed) optimization technique such as offset control [3] decides for the specific sequence of phases. We

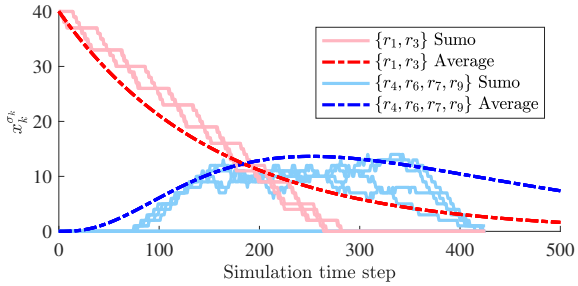

Fig. 5. Time evolution of the densities of downstream cells for the network discussed in Example 2. Comparison between a microscopic (Sumo) simulation (continuous lines), and average dynamics (dashed lines).

devote the remainder of this paper to the first stage. To formalize our optimization problem, we employ the density of the cells at roads downstream as a measure of the network congestion originated by the signalized intersections, and define the joint vector of queue lengths as

$$y_{\mathrm{av}} = C_{\mathrm{av}} x_{\mathrm{av}}, \ C_{\mathrm{av}} = \mathrm{Diag}\left\{e_{\sigma_1}^{\mathsf{T}}, \dots, e_{\sigma_{n_{\mathrm{r}}}}^{\mathsf{T}}\right\}. \tag{6}$$

We denote by x_0 the network initial state, and focus on the problem of designing the mode durations $\{d_1, \dots d_m\}$ that minimize the energy ($\mathcal{L}_2$-norm) of the queue lengths y_{av}:

$$\begin{aligned}
\min_{d_1, \dots, d_m} \quad & \int_0^\infty \|y_{\mathrm{av}}\|_2^2 \, dt \\
\text{subject to} \quad & \dot{x}_{\mathrm{av}} = A_{\mathrm{av}} x_{\mathrm{av}}, && \text{(7a)} \\
& y_{\mathrm{av}} = C_{\mathrm{av}} x_{\mathrm{av}}, && \text{(7b)} \\
& x_{\mathrm{av}}(0) = x_0, && \text{(7c)} \\
& A_{\mathrm{av}} = \frac{1}{T}\left(d_1 A_1 + \dots + d_m A_m\right), && \text{(7d)} \\
& T = d_1 + \dots + d_m, && \text{(7e)} \\
& d_i \geq 0 \quad i \in \{1, \dots, m\}. && \text{(7f)}
\end{aligned}$$

Similarly to [16], our framework focuses on the "cool down" period, where the goal is to evacuate the network as fast as possible, and where the final condition is an empty system. Thus, (7) assumes that exogenous inputs and the current network conditions enter the optimization by means of equation (7c) and through the parameters of the matrix A_{av}. Henceforth, A_{av} and the solution to (7) shall be re-computed when the exogenous inflow rates or the network traffic conditions significantly change.

III. Optimal Mode Durations Design

In this section we illustrate a numerical method for the solution of (7). The approach we introduce is centralized, namely, it requires knowledge of the state x_0 for all network cells. At its core, this technique relies on rewriting the cost function in (7) in relation to the controllability Gramian of an opportunely defined linear system, as we explain next.

Lemma 3.1: ***(Controllability Gramian cost function)*** Let

$$\mathcal{W}(A_{\mathrm{av}}, x_0) = \int_0^\infty e^{A_{\mathrm{av}} t} x_0 x_0^{\mathsf{T}} e^{A_{\mathrm{av}}^{\mathsf{T}} t} \ dt.$$

The following minimization problem is equivalent to (7):

$$\begin{aligned}\min_{d_1,\dots,d_m} \quad & \text{Trace}\left(C_{\text{av}}\ \mathcal{W}(A_{\text{av}},x_0)\ C_{\text{av}}^{\mathsf{T}}\right)\\ \text{subject to} \quad & A_{\text{av}}=\frac{1}{T}\left(d_1A_1+\cdots+d_mA_m\right),\\ & T=d_1+\cdots+d_m,\\ & d_i\geq 0,\quad i\in\{1,\dots,m\}.\end{aligned}\tag{8}$$

□

We recall that the trace of the controllability Gramian represents the energy ($\mathcal{L}_2$-norm) of the impulse response of the system to exogenous inputs [17]. Therefore, the optimal set of mode durations also minimizes the energy of the impulse response of the system with input matrix $B = x_0$.

We observe that the optimization problem (7) is feasible when there exists a choice of $\{d_1,\dots,d_m\}$ that leads to a matrix A_{av} that is Hurwitz-stable, which in turns guarantees that the cost function in (8) is finite. Recall that A_{av} is Hurwitz if $\alpha(A_{\text{av}}) < 0$, where $\alpha(A_{\text{av}}) := \sup\{\Re(s) : s \in \mathbb{C}, \det(sI - A_{\text{av}}) = 0\}$ denotes the spectral abscissa of A_{av}. We next illustrate that network stability is related to a topological property of the underlying interconnection.

Theorem 3.2: ***(Stability of optimal solutions)*** Consider a traffic network $\mathcal{N} = (\mathcal{R}, \mathcal{I})$, with $|\mathcal{D}| \neq 0$, and assume that there exists a path from every node in $\mathcal{N}$ to at least one node in $\mathcal{D}$. Let $s(r_i, r_k, \bar{t}) \neq 0$ for all $(r_i, r_k) \in \mathcal{I}$, and for some $\bar{t} \in [0, T]$. Then,

$$\alpha(A_{\text{av}}) < 0.$$

□

Our solution method relies on a generalization of the concept of spectral abscissa, namely, the smoothed spectral abscissa. For a linear time-invariant system (5)-(6), the smoothed spectral abscissa [12] is defined as the root $\tilde{\alpha} \in \mathbb{R}$ of the implicit equation

$$\text{Trace}\left(C_{\text{av}}\ \mathcal{W}(A_{\text{av}} - \tilde{\alpha}I, B)\ C_{\text{av}}^{\mathsf{T}}\right) = \epsilon^{-1},\tag{9}$$

where $\epsilon \in \mathbb{R}_{\geq 0}$. We note that $\tilde{\alpha}$ is unique [12], and, for given B and C_{av}, it is a function of ϵ and A_{av}, namely $\tilde{\alpha}(\epsilon, A_{\text{av}})$.

We let $\tilde{\alpha} = 0$ in (9), then (8) can be reformulated in terms of the smoothed spectral abscissa as follows:

$$\begin{aligned}\min_{d_1,\dots,d_m,\epsilon} \quad & \epsilon^{-1}\\ \text{subject to} \quad & A_{\text{av}}=\frac{1}{T}\left(d_1A_1+\cdots+d_mA_m\right),\\ & T=d_1+\cdots+d_m,\\ & d_i\geq 0,\quad i\in\{1,\dots,m\},\\ & \tilde{\alpha}(\epsilon,A_{\text{av}})=0,\end{aligned}\tag{10}$$

where ϵ is now an optimization variable. In what follows, we let $\{d_1^*,\dots,d_m^*,\epsilon^*\}$ be the value of the optimization parameters at optimality of (10). Problem (10) is a nonlinear optimization problem [12], because the optimization variables $\{d_1,\dots,d_m\}$ and ϵ are related by means of the nonlinear equation (9). For the solution of (10), we propose an iterative two-stage numerical optimization process. In the first stage, we fix the value of ϵ and look for a choice of $\{d_1,\dots d_m\}$ that leads to a smoothed spectral abscissa that is identically zero. In other words, we let $\epsilon = \bar{\epsilon}$, and solve the following minimization problem:

$$\begin{aligned}\min_{d_1,\dots,d_m} \quad & |\tilde{\alpha}(\bar{\epsilon},A_{\text{av}})|\\ \text{subject to} \quad & A_{\text{av}}=\frac{1}{T}\left(d_1A_1+\cdots+d_mA_m\right),\\ & T=d_1+\cdots+d_m,\\ & d_i\geq 0,\quad i\in\{1,\dots,m\}.\end{aligned}\tag{11}$$

We observe that, for every $\{\bar{d}_1,\dots,\bar{d}_m\} := \min|\tilde{\alpha}(\bar{\epsilon}, A_{\text{av}})|$, solution to (11), the resulting $\bar{A}_{\text{av}} = 1/T(\bar{d}_1A_1 + \cdots + \bar{d}_mA_m)$ satisfies $\tilde{\alpha}(\bar{\epsilon}, \bar{A}_{\text{av}}) = 0$. Thus, $\bar{A}_{\text{av}}$ represents a point in the feasible set of (10) that corresponds to a cost of congestion $\int_0^\infty \|y_{\text{av}}\|_2^2\ dt = 1/\bar{\epsilon}$. In the second stage, we perform a line-search over the parameter ϵ, where the value of ϵ is increased at every iteration until the minimizer ϵ^* is achieved. It is worth noting that the solution of (11) with $\bar{\epsilon} = \epsilon^*$ is zero, and its optimizer is $\{d_1^*,\dots,d_m^*\}$. The remainder of this section is devoted to solving (11). For ease of notation, we let $\tilde{\alpha}(\bar{\epsilon}, A_{\text{av}}) = \tilde{\alpha}_{\bar{\epsilon}}$.

The benefit of solving (11) as opposed to (10) is that we can derive an expression for the gradient of $\tilde{\alpha}_{\bar{\epsilon}}$ with respect to the mode durations $\{d_1,\dots,d_m\}$, as we explain next. In what follows, for a matrix $M = [m_{ij}] \in \mathbb{R}^{m\times n}$ we denote its vectorization as $M^{\text{v}} = [m_{11}\dots m_{m1}, m_{12}\dots m_{mn}]^{\mathsf{T}}$.

Lemma 3.3: ***(Descent direction)*** Let $\tilde{\alpha}_{\bar{\epsilon}}$ denote the unique root of (9) with $\bar{\epsilon} \in \mathbb{R}_{>0}$. Let $d = [d_1,\dots,d_m]^{\mathsf{T}}$, and let $K = [A_1^{\text{v}}\ A_2^{\text{v}}\ \dots\ A_m^{\text{v}}]$. Then,

$$\frac{\partial\tilde{\alpha}_{\bar{\epsilon}}}{\partial d} = K^{\mathsf{T}}\left(\frac{QP}{\text{Trace}\,(QP)}\right)^{\text{v}},$$

where $P \in \mathbb{R}^{n\times n}$ and $Q \in \mathbb{R}^{n\times n}$ are the (unique) solutions to the two Lyapunov equations

$$\begin{aligned}(A_{\text{av}} - \tilde{\alpha}_{\bar{\epsilon}}I)P + P(A_{\text{av}} - \tilde{\alpha}_{\bar{\epsilon}}I)^{\mathsf{T}} + x_0x_0^{\mathsf{T}} &= 0,\\ (A_{\text{av}} - \tilde{\alpha}_{\bar{\epsilon}}I)^{\mathsf{T}}Q + Q(A_{\text{av}} - \tilde{\alpha}_{\bar{\epsilon}}I) + C_{\text{av}}C_{\text{av}}^{\mathsf{T}} &= 0,\end{aligned}\tag{12}$$

and $I \in \mathbb{R}^{n\times n}$ denotes the identity matrix. □

We note that, by using the inequality $\tilde{\alpha}_{\bar{\epsilon}} \geq \alpha(A_{\text{av}})$ (see [12]), the matrix $(A_{\text{av}} - \tilde{\alpha}_{\bar{\epsilon}}I)$ is Hurwitz-stable for every A_{av}. It follows that (12) always admit unique solutions P and Q.

A gradient-descent optimization technique that relies on the expressions in Lemma 3.3 is presented in Algorithm 1. Algorithm 1 employs a fixed stepsize $\mu \in (0, 1)$, and a terminating criterion (line 13) based on the Karush-Kuhn-Tucker conditions for projection methods. The ϵ-update step, which constitutes the outer while-loop (line $2 - 16$), is then performed at each iteration of the gradient descent phase, and the line-search is terminated when $|\tilde{\alpha}_\epsilon| = 0$ cannot be achieved. To prevent the algorithm from stopping at local minimas, the gradient descent algorithm (lines $3 - 13$) is repeated over multiple feasible initial conditions $d^{(0)}$.

IV. Simulation Results

This section provides numerical simulations in support to the assumptions made in this paper, and includes discussions and demonstrations of the benefits of our methods. The

Algorithm 1: Centralized solution to (7)

Input: Matrix C_{av}, vector x_0, scalars ξ, μ
Output: $\{d_1^*, \dots d_m^*, \epsilon^*\}$ solution to (7)

Initialize: $d^{(0)}$, $\bar{\epsilon} = 0$, $k = 1$
while $\tilde{\alpha}_{\bar{\epsilon}}^{(k)} = 0$ **do**
  repeat
    Compute $\tilde{\alpha}_{\bar{\epsilon}}^{(k)}$ by solving (9);
    Find P and Q that solve:
    $(A_{\text{av}}^{(k)} - \alpha_{\bar{\epsilon}}^{(k)} I)P + P(A_{\text{av}}^{(k)} - \alpha_{\bar{\epsilon}}^{(k)} I)^{\mathsf{T}} + x_0 x_0^{\mathsf{T}} = 0$;
    $(A_{\text{av}}^{(k)} - \alpha_{\bar{\epsilon}}^{(k)} I)^{\mathsf{T}} Q + Q(A_{\text{av}}^{(k)} - \alpha_{\bar{\epsilon}}^{(k)} I) + C_{\text{av}} C_{\text{av}}^{\mathsf{T}} = 0$;
    $\frac{\partial \alpha_{\bar{\epsilon}}^{(k)}}{\partial d} \leftarrow \frac{QP}{\text{Trace}(QP)}$;
    $\nabla \leftarrow \tilde{\alpha}_{\bar{\epsilon}} \frac{\partial \alpha_{\bar{\epsilon}}^{(k)}}{\partial d}$;
    Compute projection matrix $\mathcal{P}^{(k)}$;
    $d^{(k)} \leftarrow d^{(k)} - \mu\, \mathcal{P}^{(k)} \nabla$;
    $A_{\text{av}}^{(k)} \leftarrow \frac{1}{T}(d_1 A_1 + \dots + d_m A_m)$;
    $k \leftarrow k + 1$;
  until $\mathcal{P}^{(k)} \nabla = 0$;
  $\bar{\epsilon} \leftarrow \bar{\epsilon} + \xi$;
end
return d;

proposed technique have been implemented for validation in a simulator based on *Sumo* (*Simulation of Urban MObility* [18]). We consider the network depicted in Fig. 4 and discussed in Example 2, and we consider the congestion cost associated with non-destination roads. We assume that roads $\{r_2, r_5\}$ represent destinations with higher interest, and model the network routing as $c(r_4, r_1) = c(r_4, r_3) = c(r_7, r_{10}) = c(r_7, r_{12}) = 0.7$, $c(r_6, r_1) = c(r_6, r_3) = c(r_9, r_{10}) = c(r_9, r_{12}) = 0.3$, and $c(r_i, r_j) = 0.5$ otherwise. We let the network be subject to constant exogenous inflows $u_{r_i} = 100$veh/h, for all $r_i \in \mathcal{S}$ (see Example 2). Fig. 6 shows a comparison between the trajectories of $\|y\| = \|C_{\text{av}} x\|$ for i) the solution to (7), ii) max-pressure distributed policies, and iii) a uniform choice of mode durations with $d_i = 0.5$, $i \in \{1, \dots, m\}$. The comparison illustrates the benefits in the overall network congestion when the proposed optimization technique (7) is employed. The suboptimal performance of distributed control policies can be attributed to the limited (local) knowledge of the current traffic conditions, and to the lack of availability of a global network model.

V. Conclusions

This paper describes a simplified model to capture the dynamics of traffic flows in transportation systems. This model allows us to reformulate the goal of optimizing network congestion as the problem of minimizing a metric of controllability of an opportunely-defined dynamical system associated with the network. Our results show that the availability of an approximate centralized model can considerably improve the network efficiency, and allows for a more tractable analysis compared to traditional models. We show how the performance of distributed policies deteriorate due to the lack of availability of a global network model, capable of capturing the overall network dynamics. We envision that our model of traffic network will be useful in future research targeting design of traffic networks, control, and security analysis.

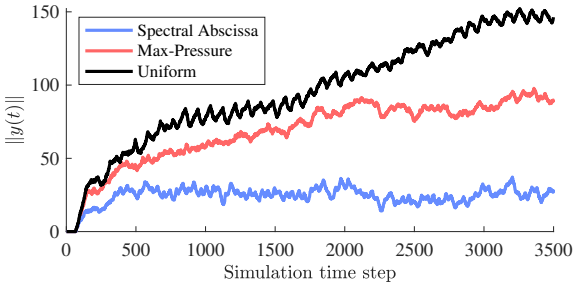

Fig. 6. Simulated time evolution of $\|y\| = \|C_{\text{av}} x\|$ for different intersection control methods.

References

[1] E. Lovisari, G. Como, A. Rantzer, and K. Savla, "Stability analysis and control synthesis for dynamical transportation networks," *arXiv preprint*, 2014.

[2] Q. Ba, K. Savla, and G. Como, "Distributed optimal equilibrium selection for traffic flow over networks," in *IEEE Conf. on Decision and Control*. IEEE, 2015, pp. 6942–6947.

[3] S. Coogan, E. Kim, G. Gomes, M. Arcak, and P. Varaiya, "Offset optimization in signalized traffic networks via semidefinite relaxation," *Transp. Research Pt. B: Methodological*, vol. 100, pp. 82–92, 2017.

[4] C. Diakaki, M. Papageorgiou, and K. Aboudolas, "A multivariable regulator approach to traffic-responsive network-wide signal control," *Control Engineering Practice*, vol. 10, no. 2, pp. 183–195, 2002.

[5] P. Hunt, D. Robertson, R. Bretherton, and M. C. Royle, "The SCOOT on-line traffic signal optimisation technique," *Traffic Engineering & Control*, vol. 23, no. 4, 1982.

[6] P. Mirchandani and L. Head, "A real-time traffic signal control system: architecture, algorithms, and analysis," *Transportation Research Part C: Emerging Technologies*, vol. 9, no. 6, pp. 415–432, 2001.

[7] N. H. Gartner, F. J. Pooran, and C. M. Andrews, "Implementation of the opac adaptive control strategy in a traffic signal network," in *IEEE Trans. on Intelligent Transp. Systems*, 2001, pp. 195–200.

[8] T. Wongpiromsarn, T. Uthaicharoenpong, Y. Wang, E. Frazzoli, and D. Wang, "Distributed traffic signal control for maximum network throughput," 2012, pp. 588–595.

[9] P. Varaiya, "The max-pressure controller for arbitrary networks of signalized intersections," in *Advances in Dynamic Network Modeling in Complex Transportation Systems*. Springer, 2013, pp. 27–66.

[10] M. Papageorgiou, C. Diakaki, V. Dinopoulou, A. Kotsialos, and Y. Wang, "Review of road traffic control strategies," *Proceedings of the IEEE*, vol. 91, no. 12, pp. 2043–2067, 2003.

[11] P. Grandinetti, C. C. de Wit, and F. Garin, "Distributed optimal traffic lights design for large-scale urban networks," *IEEE Transactions on Control Systems Technology*, pp. 1–14, 2018.

[12] J. Vanbiervliet, B. Vandereycken, W. Michiels, S. Vandewalle, and M. Diehl, "The smoothed spectral abscissa for robust stability optimization," *SIAM Journal on Optimization*, vol. 20, no. 1, 2009.

[13] C. F. Daganzo, "The cell transmission model: A dynamic representation of highway traffic consistent with the hydrodynamic theory," *Transp. Research Pt. B: Methodological*, vol. 28, no. 4, 1994.

[14] L. B. De Oliveira and E. Camponogara, "Multi-agent model predictive control of signaling split in urban traffic networks," *Transportation Research Part C: Emerging Technologies*, vol. 18, no. 1, 2010.

[15] R. Middlebrook and S. Cuk, "A general unified approach to modelling switching-converter power stages," in *Power Electronics Specialists Conference*. IEEE, 1976, pp. 18–34.

[16] G. Gomes and R. Horowitz, "Optimal freeway ramp metering using the asymmetric cell transmission model," *Transportation Research Part C: Emerging Technologies*, vol. 14, no. 4, pp. 244–262, 2006.

[17] F. Pasqualetti, S. Zampieri, and F. Bullo, "Controllability metrics, limitations and algorithms for complex networks," *IEEE Transactions on Control of Network Systems*, vol. 1, no. 1, pp. 40–52, 2014.

[18] M. Behrisch, L. Bieker, J. Erdmann, and D. Krajzewicz, "Sumo-simulation of urban mobility: an overview," in *Conf. on Advances in System Simulation*, 2011.